Asian Journal of Chemistry; Vol. 33, No. 4 (2021), 814-818

ASIAN JOURNAL OF CHEMISTRY

https://doi.org/10.14233/ajchem.2021.23082

Density Functional Theory Reactivity Studies on $X_3N@C_{80}$ (X = Sc, Gd, Lu) Fullerenes

P. SELVARENGAN

Department of Physics and International Research Centre, Kalasalingam Academy of Research and Education (Deemed to be University), Krishnankoil-626126, India

*Corresponding author: E-mail: p.selvarengan@klu.ac.in

Received: 26 November 2020; *Accepted*: 3 February 2021; *Published online*: 20 March 2021; AJC-20288

Density functional theory studies have been performed to reveal the reactivity of the sites in $Sc_3N@C_{80}$, $Gd_3N@C_{80}$ and $Lu_3N@C_{80}$ endohedral fullerenes. The condensed Fukui functions have been calculated using Mulliken atomic charges. The calculations show that the carbon atom sites are in direct contact with the endohedral cluster favourable nucleophilic attack. Similarly, the carbon atoms which are away from the direct bonding with the cluster are favourable for the electrophilic attack. This is also confirmed from the charge transfer analysis. It is noted that the spin multiplicity decides the reactivity sites and stability of the $Gd_3N@C_{80}$ system. The HOMO-LUMO gap value indicates that $Gd_3N@C_{80}$ with S = 7 is stable than the S = 21 system. Finally, present studies indicate that the charge transfer between the C_{80} cage and X_3N plays a major role to determine the reactivity of the sites in the C_{80} cage.

Keywords: DFT, Reactivity, Condensed Fukui functions, Endohedral fullerenes, Scandium, Gadolinium, Lutetium.

INTRODUCTION

Since the discovery of endohedral fullerenes in the early 90s, they have attracted great interest due to their enhanced stability and a large variety of cage sizes [1-3]. The endohedral fullerenes have been investigated for their potential application as a new contrast agent in magnetic resonance imaging (MRI) [4,5]. So far many new cluster fullerenes have been synthesized by tuning the trapped metal atoms and stabilizing a large variety of cage sizes including different isomeric structures [6-10], different types of fullerenes with encapsulating different types of metals such as alkali metal, group 2 and 3 metal as well as lanthanide have been synthesized [11,12]. Similarly, recent studies have been performed on the mixed metal-nitride cluster fullerenes. The recent progress achieved in the isolation of the mixed-metal cluster fullerenes is mainly due to difficulties in their HPLC separation. Because of cluster fullerenes with variable cluster composition but the same carbon cage isomer exhibit a very similar HPLC behaviour [13,14]. During late 90s, the experimental synthesis methods produce 0.5% and multiple endohedral fullerenes isomers that make it difficult in the studies of their properties.

The structure and electronic properties of endohedral fullerenes are well studied in both theoretically [15-19] and experimentally [20-23]. Based on scalar-relativistic DFT calculations the optical excitations of $Sc_3N@C_{80}$ and $Lu_3N@C_{80}$ metal nitride clusters are discussed [24]. An enormous amount of studies have been performed on the other metallofullerenes. Those studies were mainly concentrated on the structural, electronic, and magnetic properties. Further, earlier studies have concluded that the stability of the clusters due to the charge transfer takes place between the nitride cluster and the cage. Since the number of transferred charges is large, it may enhance the reactivity of sites in the carbon cage. However, the molecular scale information such as reactivity is not yet fully elucidated. Some studies have been performed on measuring the optical gap and electronic properties of these clusters. However, limited attention has been given to the reactivity of the sites on the cluster cages on these metalloclusters. Estrada-Salas & Valladares [16] have studied the surface reactivity of 3*d*-metal endofullerenes using the density functional theory method. They have analyzed the changes in the preferential sites of electrophilic, nucleophilic, and radical attacks on the pristine C_{60} surface with endohedral doping using 3*d*-transition metal anions. They have used two

reactivity indices, such as Fukui functions and molecular electrostatic potentials. Hence in the present study, the reactivity studies on Sc, Gd, and Lu containing C_{80} clusters using first-principles electronic structure calculations were performed. Theoretical investigations of endohedral fullerenes represent a complex task, which can be performed with sufficient accuracy with the help of the first-principles density functional theory (DFT). Special emphasis has also been given to predicting the active binding sites for the above molecules using condensed Fukui functions. Secondly, the change in the reactivity of sites in endohedral fullerenes with different spin multiplicity system was studied. For this purpose, the $Gd_3N@C_{80}$ system is selected, because water-soluble Gd-based endohedral fullerenes have attracted recent interest as a possible new generation of magnetic resonance imaging (MRI) contrast agents. They not only can produce proton relaxivities several times and even ten times greater than commercially available MRI contrast agents but also are safer than the latter because the toxic Gd ions are completely encaged inside the fullerene and do not dissociate under physiological conditions. The spin multiplicity of a single Gd^{3+} ion is 8 and the dimer is 19. Lu *et al*. [25] revealed the structure and magnetic properties of $Gd_3N@C_{80}$ using density functional theory methods. They have studied the various configurations and spin multiplicity of $Gd_3N@C_{80}$ endohedral fullerenes. Hence in the present study, the structural stability and the reactivity of the sites in C_{80} cage associated with the higher spin multiplicity of the Gd based system is performed.

COMPUTATIONAL METHODS

All the calculations were performed using the Gaussian 09W package [26]. The molecular structures of the studied clusters were optimized at the PBEPBE/def2-TZVPP method (Fig. 1). Vibrational frequency analyses were performed to identify the structure as a global minimum structure. The condensed fukui functions $f_k(r)$ have been calculated using the atomic charges q_k calculated by the Mulliken charge analysis [27,28].

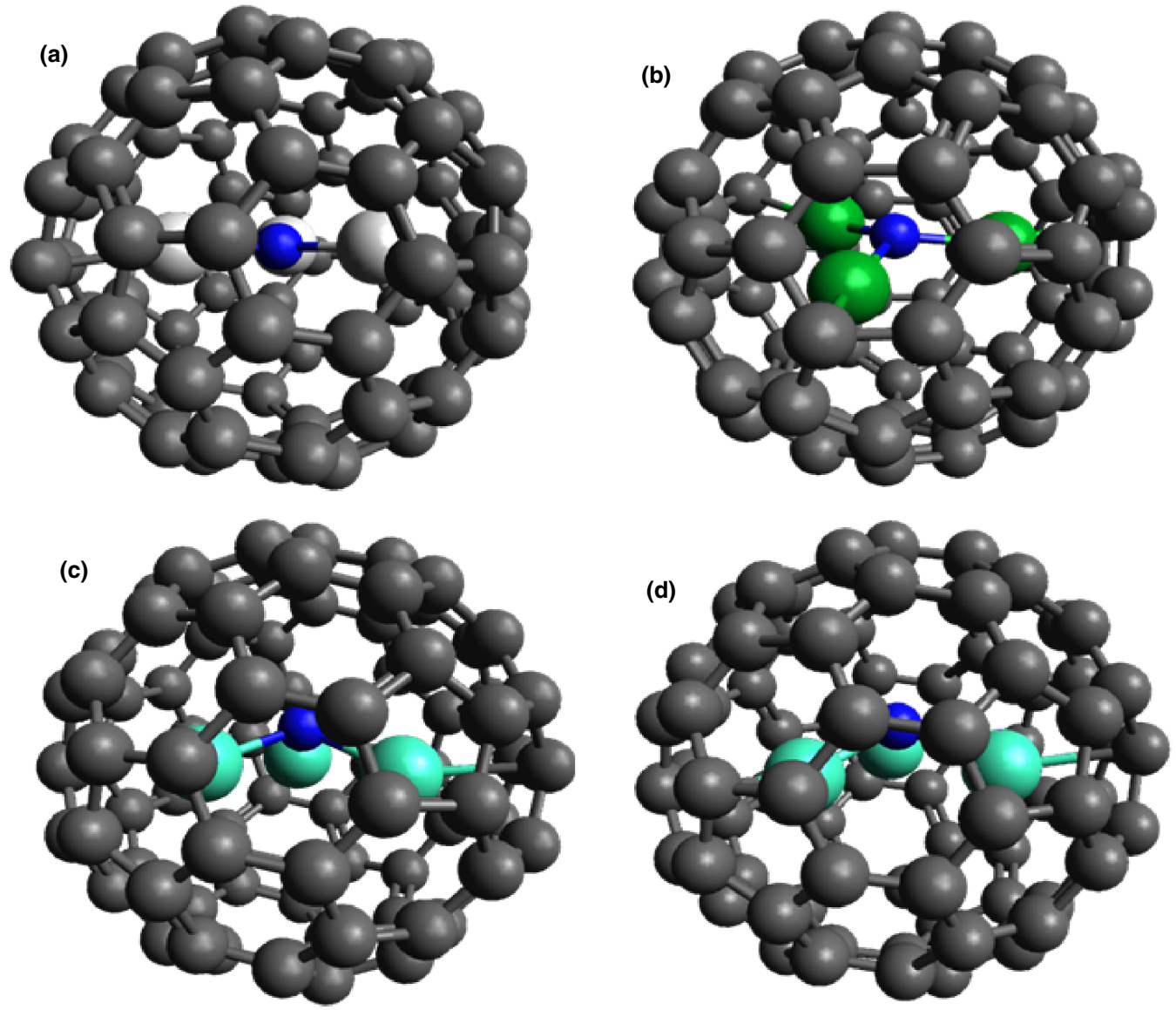

Fig. 1. Optimized structures of (a) $Sc_3N@C80$, (b) $Lu_3N@C80$ (c) $Gd_3N@C80$ (S=7) (d) $Gd_3N@C80$ (S=21) (atom colour: carbon (grey), nitrogen (blue), scandium (white), lutetium (dark green), gadolinium (light green)

$$f_k^+ = q_k(N+1) - q_k(N)$$

$$f_k^- = q_k(N) - q_k(N-1)$$

$$f_k^0 = ½[q_k(N+1) - q_k(N-1)]$$

where N refers to the number of electrons in the system K, and condensed Fukui functions f_k^+, f_k^-, and f_k^0 represent the nucleophilic, electrophilic, and radial attacks, respectively.

RESULTS AND DISCUSSION

To validate the functional and basis set used in this study, the HOMO-LUMO gap was calculated and compared it with the available experimental data. The results are shown in Table-1. The HOMO-LUMO gap is an important quantity to study the stability of the system. Yoon *et al*. [29] found that the hydrogen binding energy is generally higher if the gap between the HOMO and LUMO is lower. They studied the interaction between hydrogen molecules and metallofullerenes using the first-principle density functional theory method. In the present study, the calculated HOMO-LUMO gap theoretically was compared with available experimental results on these clusters. Compare to the other available experimental and theoretical results, the HOMO-LUMO for $Sc_3N@C_{80}$, $Lu_3N@C_{80}$, $Gd_3N@C_{80}$ (I) and $Gd_3N@C_{80}$ (II) are 1.50 eV, 1.57 eV, 1.41 eV and 1.33 eV, respectively. The experimental energy gap derived from the onset of optical absorption 1.51 eV, 1.65 eV and 1.59 eV for $Sc_3N@C_{80}$, $Lu_3N@C_{80}$, and $Gd_3N@C_{80}$, respectively [30]. In comparison with available experimental results, the function used in this study produces a slightly lesser HOMO-LUMO gap value. However, it is well known that the DFT methods underestimate the HOMO-LUMO gap. Similarly, Lu *et al*. [25] used GGA+U functional for their study on magnetic properties of $Gd_3N@C_{80}$ system. Since, there is no experimental HOMO-LUMO gap available for the $Gd_3N@C_{80}$ (II) system, when compared herewith the available theoretical results of 1.33 eV, which coincides with our theoretical results.

The Fukui function proposed by Yang *et al*. [31] is one of the local reactivity indices that represent the system's response to a simultaneous perturbation in the total number of electrons N and the external potential v(r) due to the compensating positive (nuclear) charges in the system. The evaluation of the Fukui function values is not straight-forward due to the difficulties associated with solving the derivatives of electron density. Hence, Yang & Mortier [32] proposed a simple approach to calculate the site reactivity, that is, condensed Fukui functions. They have used atomic charges to determine the reactivity of the sites in the molecular systems.

In present study, condensed Fukui functions was calculated using the Mulliken population scheme and the reactive sites for the nucleophile and electrophilic attacks have been determined. The favourable reactive sites for nucleophilic (blue) and electrophilic (pink) attacks in $Sc_3N@C_{80}$, $Lu_3N@C_{80}$, $Gd_3N@C_{80}$ (I) and $Gd_3N@C_{80}$ (II) are shown in Fig. 2. It is noted that the C_{80} cage consists of pentane and hexane rings and also, as mentioned by earlier studies, the C_{80} cage contains four different types of C-C bonds in IPR fullerenes and two additional types found in non-IPR systems. In both $Sc_3N@C_{80}$ and $Lu_3N@C_{80}$ systems have similar nucleophilic and electrophilic reactive sites, *i.e*., the carbon atoms which are bonded with metal atoms favourable for the nucleophilic attack and the carbon atoms away from direct bonding with Sc or Lu were favourable for electrophilic attacks. While considering the reactivity of the sites in $Gd_3N@C_{80}$ (I) and $Gd_3N@C_{80}$ (II) systems, the reactivity of the sites in $Gd_3N@C_{80}$ (II) similar to $Sc_3N@C_{80}$ and $Lu_3N@C_{80}$ systems. However, $Gd_3N@C_{80}$ (I) system contains similar reactivity sites for the nucleophilic attack, which is the carbon atoms attached with metal atoms, favourable for nucleophilic attacks and the electrophilic attack, the reactivity of the sites were slightly different from other studied systems. If the spin multiplicity of the system is changed from 8 to 22, some of the carbon sites were turned to be favourable for electrophilic attacks. As noted in Fig. 2, some of the carbon sites were turned to be favourable electrophilic attack reactive sites, when the spin multiplicity of the system changed, while considering the number of reactive sites for nucleophilic attack and electrophilic attack, the $Sc_3N@C_{80}$ system has 5 sites are favourable for the nucleophilic attack and 12 sites are favourable for the electrophilic attack, similarly for $Lu_3N@C_{80}$ system has 6 sites and 12 sites for nucleophilic and electrophilic attacks respectively. In $Gd_3N@C_{80}$ (I) system, the number of carbon sites is 6 and 5 for nucleophilic and electrophilic attacks. In the $Gd_3N@C_{80}$ (II) system, the number of carbon sites is 6 and 9 sites favourable for nucleophilic and electrophilic attacks. Overall, it has been noted that in the studied systems, there are 5 to 6 sites favourable for nucleophilic attacks and varies from 5 to 12 sites favourable for electrophilic attacks. This indicates that most of the studied systems were favourable for electrophilic attacks, except $Gd_3N@C_{80}$ (I) system where the number of reactive sites were almost equal.

Dipole moment is a quantity that measures the system stability in the liquid phase. The dipole moment of the studied systems *viz*. Sc_3N, $Gd_3N@C_{80}$ (I), $Gd_3N@C_{80}$ (II) and $Lu_3N@C_{80}$ endohedral fullerenes are given in Table-1. The large values of the $Gd_3N@C_{80}$ system are due to the dipole moment pointing towards the z-direction. This large value indicates the system stability in the liquid phase. Based on the dipole moment values, in comparison with other studied systems, the Gd based system could be more stable in the liquid phase. Because the electro-

TABLE-1
CALCULATED HOMO-LUMO (HL) GAP, DIPOLE MOMENT (D), ELECTRON AFFINITY (EA) AND DIHEDRAL ANGLE

Parameters	$Sc_3N@C_{80}$	$Lu_3N@C_{80}$	$Gd_3N@C_{80}$ (S = 7)	$Gd_3N@C_{80}$ (S = 21)
HOMO-LUMO (eV)	1.50	1.57	1.41	1.33
Dipole moment (debye)	0.203	0.410	1.109	1.105
Electron affinity (eV)	4.21	4.22	4.39	4.44
Dihedral angle <N-X1-X2-X3>	-0.630	-16.010	-35.640	-35.830

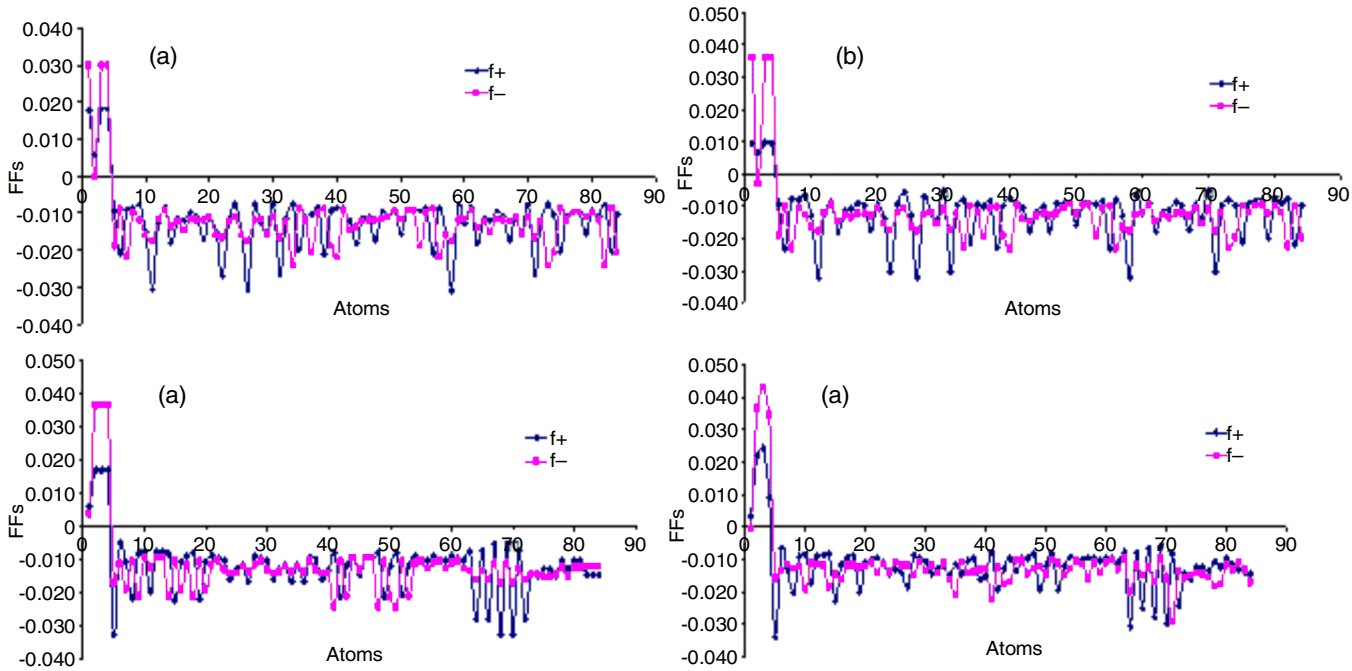

Fig. 2. Condensed Fukui functions of (a) $Sc_3N@C_{80}$, (b) $Lu_3N@C_{80}$, (c) $Gd_3N@C_{80}$ (S=7) and (d) $Gd_3N@C_{80}$ (S=21)

static forces are long-range forces, which play a crucial role in defining the structures and properties of the system [33]. The above force arises due to the presence of the permanent electric dipole moments in the structure. In present study, the large dipole moment of $Gd_3N@C_{80}$ fullerene could be arising due to the floppiness of the endohedral X_3N. The calculated electron affinity values of Sc and Lu based fullerenes have similar values and it is noted that around 0.056 eV difference between the $Gd_3N@C_{80}$ (I) and $Gd_3N@C_{80}$ (II) system. The large electron affinity value was noted at $Gd_3N@C_{80}$ (II) endohedral fullerene.

The atomic charges of the studied systems have been calculated using the Mulliken population. In the Raman spectrum, the low-energy part of the vibrational pattern was studied, since it is directly correlated to bond formation between the M_3N cluster and fullerene cage. All the studied systems were found to be neutral. It has been noted that the total charge of endohedral X_3N group is slightly positive because the inner group contains three metal ions and one electronegative atom. The C80 cage is slightly negative in all the studied systems (Table-2). The C_{80} cage of Sc doped system is less negative (-1.105 e), and Lu doped system is more negative (-1.394 e). This indicates that the inner group Lu_3N gains a more positive charge which leads the C_{80} cage more negative. As mentioned by Yang *et al.* [34], the smaller cluster-cage force constant in $Sc_3N@C_{80}$ than the other studied system could be the reason behind lesser charge transfer in Sc based system (Table-2). While considering both Gd_3N systems, there are no significant changes in the charges of the inner group and cage. The negative charges of the C_{80} group of all the studied systems indicate that the cage attracts the electron-deficient system that is, electrophile towards the surface. While comparing all the studied system, Lu based endohedral fullerene is more favourable for the electrophilic attack, which is due to the higher negative charge at the surface. These large charges transferred to the cage will localize on the surface and that enhance the reactivity of these carbon sites for the electrophile attack.

TABLE-2
MULLIKEN CHARGE TRANSFER IN $Sc_3N@C_{80}$, $Lu_3N@C_{80}$, $Gd_3N@C_{80}$ (S = 7), $Gd_3N@C_{80}$ (S = 21)

Parameters	$Sc_3N@C_{80}$	$Lu_3N@C_{80}$	$Gd_3N@C_{80}$ (S = 7)	$Gd_3N@C_{80}$ (S = 21)
X1	0.533	0.641	0.538	0.537
X2	0.533	0.641	0.537	0.537
X3	0.533	0.641	0.536	0.537
N	-0.493	-0.527	-0.477	-0.476
C80	-1.105	-1.394	-1.132	-1.134

The spin density is a property that also contains information about the reactivity of the molecular system. Because the large spin moment of Gd-based endohedral fullerene revealed that, the alignment of the spin moment could provide insights about the reactivity of the system. In present study, we have studied the spin multiplicity 8 and 22 systems. In the $Gd_3N@C_{80}$ (I) system, the spin moment of the three Gd atoms was not aligned parallel that is antiferromagnetic, whereas, in the $Gd_3N@C_{80}$ (II) system, the spin moment of all the Gd atoms were aligned parallel, *i.e.* ferromagnetic nature. This could play the important role in the different reactivity of the sites for the electrophilic attack in these systems.

Conclusion

In the present investigation, density functional theory calculations were performed to study the structure and reactivity of $X_3N@C80$ (X = Sc, Lu, Gd) endohedral fullerenes. The calculations have shown that the studied endohedral fullerenes have a HOMO-LUMO gap value around 1.5 eV. The calculated HOMO-LUMO gap of the studied systems has slightly lower than the experimental value. The condensed Fukui functions have shown that the reactivity of the sites is similar

in Sc and Lu system. However, in the case of Gd system with spin 7 and 21, the reactivity of the site significantly changed. The dipole moment values indicate that the Gd-based endohedral fullerenes are stable in the liquid phase. This shows that the Gd based endohedral fullerenes can be used in magnetic resonance imaging. Further, it can be noted that the charge transfer between X_3N and C_{80} cage plays an important role to determine the reactivity of the site.

ACKNOWLEDGEMENTS

The author is thankful to the Management of Kalasalingam Academy of Research and Education, for providing the financial support to establish a computational research facility at the International Research Centre, Kalasalingam Academy of Research and Education, Krishnankoil, India.

CONFLICT OF INTEREST

The authors declare that there is no conflict of interests regarding the publication of this article.

REFERENCES

1. A.A. Popov, S. Yang and L. Dunsch, *Chem. Rev*., **113**, 5989 (2013); https://doi.org/10.1021/cr300297r
2. S. Wang, Q. Chang, G. Zhang, F. Li, X. Wang, S. Yang and S.I. Troyanov, *Front. Chem.*, **8**, 607712 (2020); https://doi.org/10.3389/fchem.2020.607712
3. D.S. Bethune, R.D. Johnson, J.R. Salem, M.S. De Vries and C.S. Yannoni, *Nature*, **366**, 123 (1993); https://doi.org/10.1038/366123a0
4. C.Y. Shu, C.R. Wang, J.F. Zhang, H.W. Gibson, H.C. Dorn, F.D. Corwin, P.P. Fatouros and T.J.S. Dennis, *Chem. Mater.*, **20**, 2106 (2008); https://doi.org/10.1021/cm7023982
5. J. Zhang, Y. Ye, Y. Chen, C. Pregot, T. Li, S. Balasubramaniam, D.B. Hobart, Y. Zhang, S. Wi, R.M. Davis, L.A. Madsen, J.R. Morris, S.M. LaConte, G.T. Yee and H.C. Dorn, *J. Am. Chem. Soc.*, **136**, 2630 (2014); https://doi.org/10.1021/ja412254k
6. M.M. Olmstead, A. de Bettencourt-Dias, J.C. Duchamp, S. Stevenson, D. Marciu, H.C. Dorn and A.L. Balch, *Angew. Chem. Int. Ed.*, **40**, 1223 (2001); https://doi.org/10.1002/1521-3773(20010401)40:7<1223::AID-ANIE1223>3.0.CO;2-B
7. M.M. Olmstead, A. de Bettencourt-Dias, J.C. Duchamp, S. Stevenson, H.C. Dorn and A.L. Balch, *J. Am. Chem. Soc*., **122**, 12220 (2000); https://doi.org/10.1021/ja001984v
8. C.M. Beavers, T. Zuo, J.C. Duchamp, K. Harich, H.C. Dorn, M.M. Olmstead and A.L. Balch, *J. Am. Chem. Soc*., **128**, 11352 (2006); https://doi.org/10.1021/ja063636k
9. N. Chen, C.M. Beavers, M. Mulet-Gas, A. Rodríguez-Fortea, E.J. Munoz, Y.Y. Li, M.M. Olmstead, A.L. Balch, J.M. Poblet and L. Echegoyen, *J. Am. Chem. Soc.*, **134**, 7851 (2012); https://doi.org/10.1021/ja300765z
10. S. Caliskan, *J. Clust. Sci.*, **32**, 77 (2020); https://doi.org/10.1007/s10876-020-01762-2
11. H. Shinohara, *Rep. Prog. Phys.*, **63**, 843 (2000); https://doi.org/10.1088/0034-4885/63/6/201
12. M. Takata, E. Nishibori, M. Sakata and H. Shinohara, Fullerene-Based Materials, Springer, pp 59-84 (2004).
13. L. Dunsch and S. Yang, *Small*, **3**, 1298 (2007); https://doi.org/10.1002/smll.200700036
14. L. Dunsch and S. Yang, *Phys. Chem. Chem. Phys.*, **9**, 3067 (2007); https://doi.org/10.1039/B704143H
15. R.E. Estrada-Salas and A.A. Valladares, *J. Mol. Struct. THEOCHEM*, **869**, 1 (2008); https://doi.org/10.1016/j.theochem.2008.08.017
16. R.E. Estrada-Salas and A.A. Valladares, *J. Phys. Chem. A*, **113**, 10299 (2009); https://doi.org/10.1021/jp9029979
17. M. Chi, P. Han, X. Fang, W. Jia, X. Liu and B. Xu, *J. Mol. Struct. THEOCHEM*, **807**, 121 (2007); https://doi.org/10.1016/j.theochem.2006.12.020
18. A. Pahuja and S. Srivastava, *Int. J. Mod. Phys. B*, **27**, 1350152 (2013); https://doi.org/10.1142/S021797921350152X
19. W. Fu, J. Zhang, H. Champion, T. Fuhrer, H. Azuremendi, T. Zuo, J. Zhang, K. Harich and H.C. Dorn, *Inorg. Chem.*, **50**, 4256 (2011); https://doi.org/10.1021/ic101772d
20. S. Guha and K. Nakamoto, *Coord. Chem. Rev.*, **249**, 1111 (2005); https://doi.org/10.1016/j.ccr.2004.11.017
21. S. Iida, Y. Kubozono, Y. Slovokhotov, Y. Takabayashi, T. Kanbara, T. Fukunaga, S. Fujiki, S. Emura and S. Kashino, *Chem. Phys. Lett.*, **338**, 21 (2001); https://doi.org/10.1016/S0009-2614(01)00234-2
22. S. Stevenson, G. Rice, T. Glass, K. Harich, F. Cromer, M.R. Jordan, J. Craft, E. Hadju, R. Bible, M.M. Olmstead, K. Maitra, A.J. Fisher, A.L. Balch and H.C. Dorn, *Nature*, **401**, 55 (1999); https://doi.org/10.1038/43415
23. I.E. Kareev, V.P. Bubnov, E.K. Alidzhanov, S.N. Pashkevich, Y.D. Lantukh, S.N. Letuta and D.A. Razdobreev, *Phys. Solid State*, **62**, 206 (2020); https://doi.org/10.1134/S1063783420010163
24. S. Osuna, R. Valencia, A. Rodríguez Fortea, M. Swart, M. Solà and J.M. Poblet, *Chem. Eur. J.*, **18**, 8944 (2012); https://doi.org/10.1002/chem.201200940.
25. J. Lu, R.F. Sabirianov, W.N. Mei, Y. Gao, C.G. Duan and X.C. Zeng, *J. Phys. Chem. B*, **110**, 23637 (2006); https://doi.org/10.1021/jp0662395
26. M.J. Frisch, G.W. Trucks, H.B. Schlegel, G.E. Scuseria, M.A. Robb, J.R. Cheeseman, G. Scalmani, V. Barone, B. Mennucci, G.A. Petersson, H. Nakatsuji, M. Caricato, X. Li, H.P. Hratchian, A.F. Izmaylov, J. Bloino, G. Zheng, J.L. Sonnenberg, M. Hada, M. Ehara, K. Toyota, R. Fukuda, J. Hasegawa, M. Ishida, T. Nakajima, Y. Honda, O. Kitao, H. Nakai, T. Vreven, J.A. Montgomery Jr., J.E. Peralta, F. Ogliaro, J.J. Heyd, M. Bearpark, J.E. Brothers, K.N. Kudin, V.N. Staroverov, R. Kobayashi, J. Normand, K. Raghavachari, A. Rendell, J.C. Burant, S.S. Iyengar, J. Tomasi, M. Cossi, N. Rega, J.M. Millam, M. Klene, J.E. Knox, J.B. Ross, V. Bakken, C. Adamo, J. Jaramillo, R. Gomperts, R.E. Stratmann, O. Yazyev, A.J. Austin, R. Cammi, C. Pomelli, J.W. Ochterski, R.L. Martin, K. Morokuma, V.G. Zakrzewski, G.A. Voth, P. Salvador, J.J. Dannenberg, S. Dapprich, A.D. Daniels, O. Farkas, J.B. Foresman, J.V. Ortiz, J. Cioslowski and D.J. Fox, Gaussian 09, Revision D.01; Gaussian Wallingford, CT (2009).
27. P. Fuentealba, P. Pérez and R. Contreras, *J. Chem. Phys.*, **113**, 2544 (2000); https://doi.org/10.1063/1.1305879
28. P. Bultinck, S. Fias, C. Van Alsenoy, P.W. Ayers and R. Carbó-Dorca, *J. Chem. Phys.*, **127**, 34102 (2007); https://doi.org/10.1063/1.2749518
29. M. Yoon, S. Yang and Z. Zhang, *J. Chem. Phys.*, **131**, 64707 (2009); https://doi.org/10.1063/1.3197006
30. Y. Zhu, Y. Li and Z.Q. Yang, *Chem. Phys. Lett.*, **461**, 285 (2008); https://doi.org/10.1016/j.cplett.2008.07.045
31. W. Yang, R.G. Parr and R. Pucci, *J. Chem. Phys.*, **81**, 2862 (1984); https://doi.org/10.1063/1.447964
32. W. Yang and W.J. Mortier, *J. Am. Chem. Soc.*, **108**, 5708 (1986); https://doi.org/10.1021/ja00279a008
33. P. Kolandaivel, P. Selvarengan and K.V. Gunavathy, *Biochim. Biophys. Acta. Proteins Proteomics*, **1764**, 138 (2006); https://doi.org/10.1016/j.bbapap.2005.10.016
34. S. Yang, S.I. Troyanov, A.A. Popov, M. Krause and L. Dunsch, *J. Am. Chem. Soc.*, **128**, 16733 (2006); https://doi.org/10.1021/ja066814i